Recent results from the NA49 experiment

2008 J. Phys. G: Nucl. Part. Phys. 35 044004

(http://iopscience.iop.org/0954-3899/35/4/044004)

IOP PUBLISHING JOURNAL OF PHYSICS G: NUCLEAR AND PARTICLE PHYSICS

J. Phys. G: Nucl. Part. Phys. **35** (2008) 044004 (7pp) doi:10.1088/0954-3899/35/4/044004

Recent results from the NA49 experiment

Christoph Blume (for the NA49 Collaboration[1])

Institut für Kernphysik der J.W. Goethe Universität, 60438 Frankfurt am Main, Germany

Received 28 September 2007
Published 17 March 2008
Online at stacks.iop.org/JPhysG/35/044004

Abstract

Recent results from the NA49 experiment at the CERN-SPS are discussed. These include new data on proton and (anti)-proton production at different beam energies, which allow us to study the energy dependence of stopping. Also, new data on the system size dependence of hyperon production at 40A and 158A GeV, on global Λ polarization, on elliptic flow of strange particles and on high-p_t nuclear suppression factors are presented.

(Some figures in this article are in colour only in the electronic version)

1. Introduction

The NA49 experiment is a fixed target experiment at the CERN-SPS. Details on the experimental setup can be found in [1]. In the recent years NA49 has collected data on nucleus–nucleus collisions at several different beam energies between 20A and 158A GeV with the objective to cover the critical region of energy densities where the expected phase transition from a deconfined phase might occur in the early stage of the reactions. Also, the system size dependence of various hadronic observables has been studied by investigating minimum bias Pb+Pb and central C+C and Si+Si collisions at 40A and 158A GeV.

2. Energy dependence of stopping

Figure 1 summarizes new results on the rapidity spectra of protons and antiprotons in central Pb+Pb collisions at 20A–80A GeV. The data points at mid-rapidity are already published measurements for time-of-flight identified particles [2], while the results at forward rapidities are still preliminary and are based on particle identification via energy loss measurements in the TPCs. All spectra are corrected for feed down from weak decays. While the antiproton spectra do not exhibit a drastic change of spectral shape, the proton spectra show a clear evolution with beam energy.

Based on the measured rapidity spectra for p, $\bar{\mathrm{p}}$, Λ, $\bar{\Lambda}$, Ξ^- and $\bar{\Xi}^+$, the net-baryon distributions $\mathrm{d}N_{(\mathrm{B}-\bar{\mathrm{B}})}/\mathrm{d}y$ are constructed at 20A–80A GeV. The contribution of unmeasured

[1] A list of members of the NA49 Collaboration is given at the end of this issue.

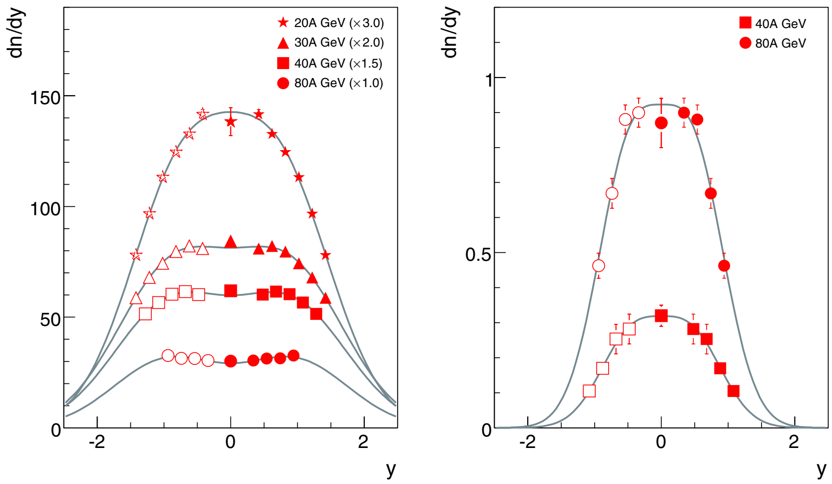

Figure 1. The rapidity spectra of protons (left panel) and antiprotons (right panel) at different beam energies in central Pb+Pb collisions. Filled symbols represent the measurements, while open symbols denote the data points selected at mid-rapidity. The lines represent the result of a fit with the sum of two Gaussians.

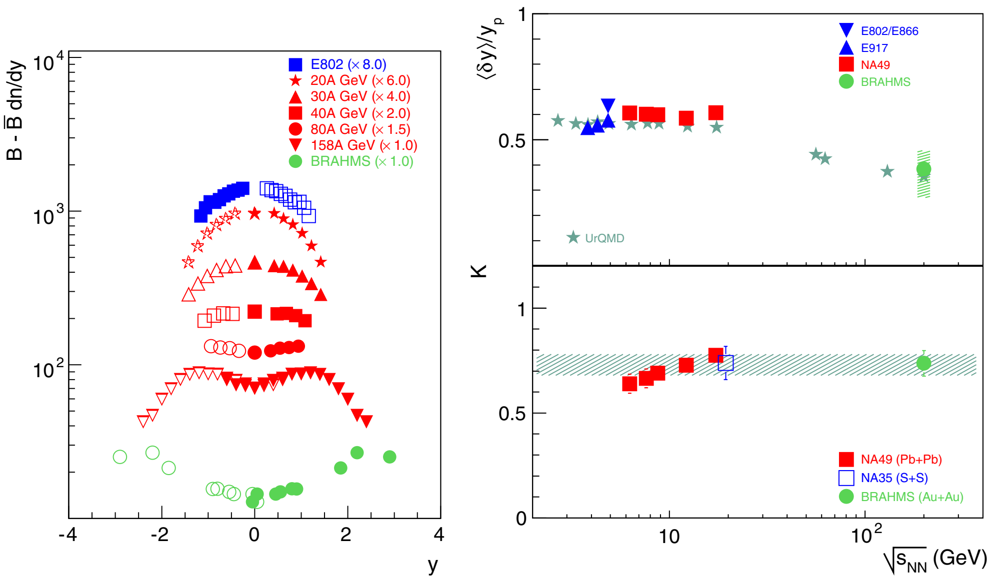

Figure 2. Left panel: the rapidity distributions of net-baryons at SPS energies [3] together with results from the AGS [5] and from RHIC [6] for central Pb+Pb(Au+Au) collisions. Right panel: the relative rapidity shift $\langle \delta y \rangle / y_{\mathrm{p}}$ as a function of the projectile rapidity y_{p} [3, 6–8] (upper part). Also shown are results for the UrQMD model [9]. The lower part summarizes the $\sqrt{s_{\mathrm{NN}}}$ dependence of the inelasticity K, including NA35 data for central S+S reactions [10].

baryons (n, $\Sigma^{\pm}$, Ξ^{0}) is estimated using the results of a statistical hadron gas model [4], assuming the same spectral shapes as for $\mathrm{p} - \bar{\mathrm{p}}$, $\Lambda - \bar{\Lambda}$ and $\Xi^{-} - \bar{\Xi}^{+}$. A transition of the spectral shape of the net-baryon distributions from a single peak to a double peak structure

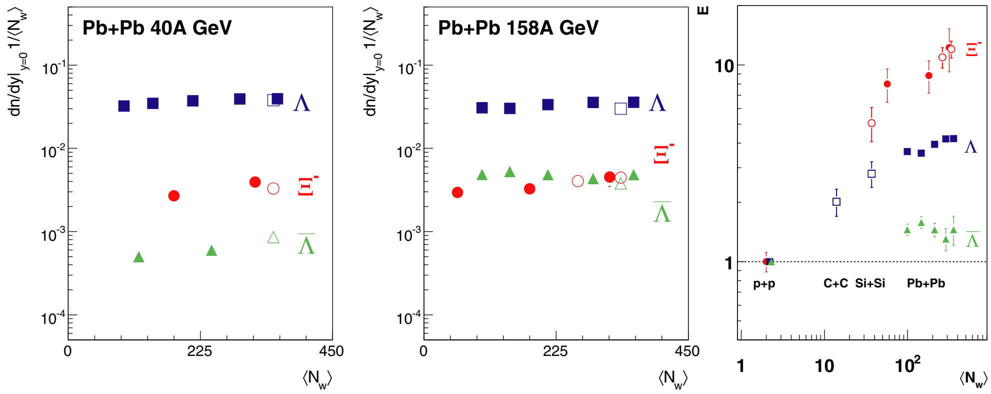

Figure 3. The rapidity densities per wounded nucleon of Λ, $\bar{\Lambda}$ and Ξ^- at midrapidity ($|y| < 0.4$ for $\Lambda(\bar{\Lambda})$, $|y| < 0.5$ for Ξ^-) for minimum bias Pb+Pb collisions (filled symbols) as a function of $\langle N_w \rangle$. Open symbols represent the results for online selected central reactions. Data are shown for 40A GeV (left panel) and 158A GeV (middle panel). Right panel: the midrapidity yields per wounded nucleon relative to p+p yields for central C+C, Si+Si and minimum bias Pb+Pb reactions at 158A GeV.

with a dip at mid-rapidity can be observed at SPS energies (see figure 2 left). This dip at $\sqrt{s_{NN}} = 17.3$ GeV evolves then further towards a shallow valley at $\sqrt{s_{NN}} = 200$ GeV. From these distributions, an averaged rapidity shift $\langle \delta y \rangle$ can be derived

$$\langle \delta y \rangle = y_p - \frac{2}{N_{\mathrm{part}}} \int_0^{y_p} y \, \frac{\mathrm{d}N_{(\mathrm{B}-\bar{\mathrm{B}})}}{\mathrm{d}y} \, \mathrm{d}y, \tag{1}$$

where y_p is the projectile rapidity and N_{part} is the number of participating nucleons. At AGS and SPS energies, a value of $\langle \delta y \rangle / y_p \approx 0.6$ is observed, which drops to $\langle \delta y \rangle / y_p \approx 0.4$ at $\sqrt{s_{NN}} = 200$ GeV (see figure 2 right). The measurements agree quite well with the UrQMD model [9]. Using $\mathrm{d}N_{(\mathrm{B}-\bar{\mathrm{B}})}/\mathrm{d}y$ and the measured $\langle m_t \rangle$ the inelastic energy per net-baryon

$$E_{\mathrm{inel}} = \frac{\sqrt{s_{NN}}}{2} - \frac{1}{N_{(\mathrm{B}-\bar{\mathrm{B}})}} \int_{-y_p}^{y_p} \langle m_t \rangle \frac{\mathrm{d}N_{(\mathrm{B}-\bar{\mathrm{B}})}}{\mathrm{d}y} \cosh y \, \mathrm{d}y \tag{2}$$

and the inelasticity $K = 2\, E_{\mathrm{inel}}/(\sqrt{s_{NN}} - 2m_p)$ can be calculated. It is found that K is approximately independent of centre-of-mass energy in the range discussed here with a value of $K \approx 0.7$–0.8 (see right panel of figure 2).

3. System size dependence of hyperon production

Figure 3 shows new NA49 results on Λ and $\bar{\Lambda}$ production in minimum bias Pb+Pb reactions at 40A and 158A GeV, together with preliminary data on Ξ^- [11]. The Λ and $\bar{\Lambda}$ data are corrected for feed down from weak decays. While there is no system size dependence of the rapidity densities per wounded nucleon for Λ and $\bar{\Lambda}$, a weak rise can be observed in the case of the Ξ^-. In combination with measurements of yields in p+p, central C+C and Si+Si [12] the system size dependence of the enhancement factor E, defined as

$$E = \left(\frac{1}{\langle N_w \rangle} \frac{\mathrm{d}N(\mathrm{Pb+Pb})}{\mathrm{d}y} \bigg|_{y=0} \right) \bigg/ \left(\frac{1}{2} \frac{\mathrm{d}N(\mathrm{p+p})}{\mathrm{d}y} \bigg|_{y=0} \right) \tag{3}$$

can be studied (rightmost panel of figure 3). $\langle N_w \rangle$ has been determined using the Glauber model [13]. The enhancement exhibits a clear hierarchy ($E(\Xi^-) > E(\Lambda) > E(\bar{\Lambda})$) and is

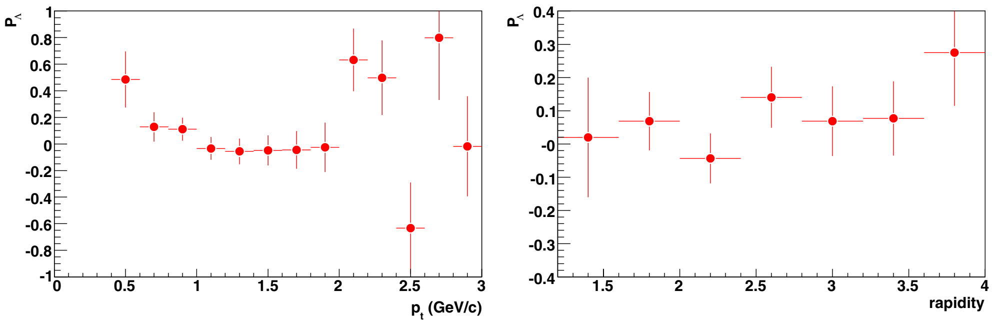

Figure 4. The global Λ polarization P_Λ as a function of p_t (left panel) and rapidity (right panel) for mid-central (12.5–43.5%) Pb+Pb collisions at 158A GeV. Only statistical errors are shown.

almost independent of the system size for $\langle N_w \rangle > 40$ for Λ and $\bar{\Lambda}$. For Ξ^- a moderate $\langle N_w \rangle$ dependence is seen. Similar trends has been observed by the NA57 collaboration, however relative to a p+Be baseline [14]. Since already in p+A reactions a slight enhancement of strange particle production is observed [16], the enhancement relative to p+Be is less. However, both SPS measurements show an enhancement that is significantly larger than that observed at $\sqrt{s_{NN}} = 200$ GeV [15].

4. Global Λ polarization

In a quark–gluon plasma state the (anti-)quarks can be polarized due to the coupling of the quark spins to the total orbital momentum $\vec{L}$ of a non-central collision system. This polarization might survive hadronization and would thus be observable as a global polarization of the measured hadrons relative to $\vec{L}$ [17]. Here we report on a measurement of the global Λ polarization P_Λ in minimum bias Pb+Pb reactions at 158A GeV. This measurement is based the following relation [19]:

$$P_\Lambda = \frac{8}{\pi \alpha_H} \frac{\left\langle \sin\left(\phi_p^* - \Psi_{EP}^{(1)}\right)\right\rangle}{R_{EP}^{(1)}}. \tag{4}$$

Here α_H is the Λ decay parameter. In this procedure, the direction of $\vec{L}$ is assumed to be normal to the reaction plane. Since this requires also the determination of the sign of $\vec{L}$, the reaction plane orientation is estimated via a measurement of the first order event plane angle $\Psi_{EP}^{(1)}$ and its resolution $R_{EP}^{(1)}$, as described in [18]. ϕ_p^* is defined as the azimuthal angle of the Λ decay proton 3-momentum in the Λ rest frame. Figure 4 shows the resulting values for P_Λ as a function of p_t and rapidity. With the possible exception of the p_t region below 0.6 GeV/c, no significant global polarization can be observed in minimum bias Pb+Pb collisions at 158A GeV, similar to the result of a comparable analysis done at $\sqrt{s_{NN}} =$ 200 GeV [19].

5. Elliptic flow

Figure 5 summarizes recent results on the elliptic flow of strange particles (Λ and K_S^0) [20] in comparison to previously published v_2 values for protons and charged pions [18]. A clear mass hierarchy of v_2 is observed: $v_2(\pi) > v_2(K_S^0) \approx v_2(p) > v_2(\Lambda)$. Such kind of

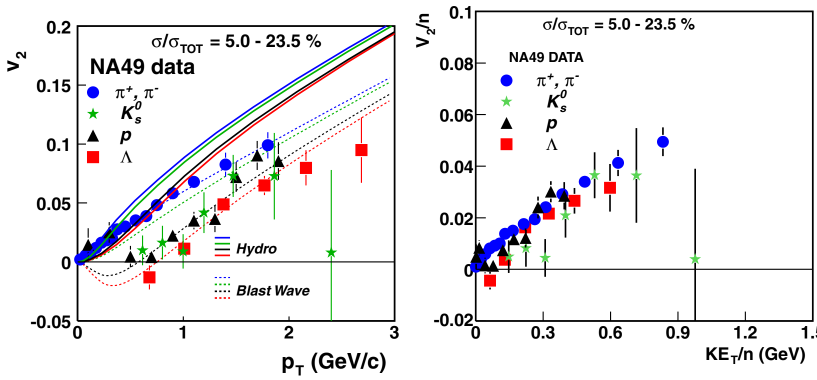

Figure 5. Left: elliptic flow v_2 for charged pions, K^0_S, protons and Λ as a function of p_t in semi-peripheral Pb+Pb collisions at 158*A* GeV. The solid lines are the results of a hydrodynamical model with $T_f = 120$ MeV, while the dashed lines represent the outcome of a blast wave fit. Right: the same data after division by the number of constituent quarks n versus the scaled transverse kinetic energy KE_t/n.

hierarchy is expected in a hydrodynamical picture, as indicated by the solid lines in the left panel of figure 5. However, the calculation shown here, assuming ideal hydrodynamics with a freeze-out temperature of $T_f = 120$ MeV [21], overpredicts the observed v_2 values. The more simpler blast wave approach [22], on the other hand, is able to describe the data reasonably well with a freeze-out temperature of $T_f = 90$ MeV and an averaged transverse flow rapidity $\langle\rho\rangle = 0.5$. At RHIC a striking scaling of v_2 at higher p_t has been observed when both v_2 and p_t are divided by the number of constituent quarks n [23]. This observation is commonly interpreted as an indication for quark coalescence as the dominating hadronization mechanism. An almost perfect scaling over the whole p_t range was achieved by plotting v_2/n versus the scaled transverse kinetic energy $KE_t/n = (m_t - m_0)/n$ [24, 25]. The right panel of figure 5 shows v_2/n versus KE_t/n for the data at SPS. In the $m_t - m_0$ range covered by NA49, the scaling seems to work to a certain extent for pions, K^0_S, Λ and protons. However, the $m_t - m_0$ reach of the NA49 data is not sufficient to answer the question whether a similar v_2/n-scaling in the high-p_t region, where v_2/n reaches a plateau, is present at SPS energies as observed at RHIC.

6. High p_t

In order to establish whether any kind of modification in the high p_t region is present in A+A collisions at SPS energies, reference data from p+p and/or p+A collisions are of high importance. Unfortunately, there are no p+p data available at $\sqrt{s} = 17.3$ GeV that cover the interesting p_t region above 2 GeV/c. Recently, the NA49 experiment has published charged pion spectra measured at this center-of-mass energy [26], but the statistics limits the p_t reach to 2.1 GeV/c. Several attempts have been made to replace the missing data by an interpolation from lower and higher beam energies [27–29]. However, one should keep in mind that at the center-of-mass energies under discussion here, the spectral shape in the higher p_t region (i.e. above $p_t = 2$ GeV/c) changes drastically with energy since the kinematic limit becomes important here. Therefore, any parametrization introduces a large systematic error. In order to overcome this current limitation, one can either use peripheral nucleus–nucleus

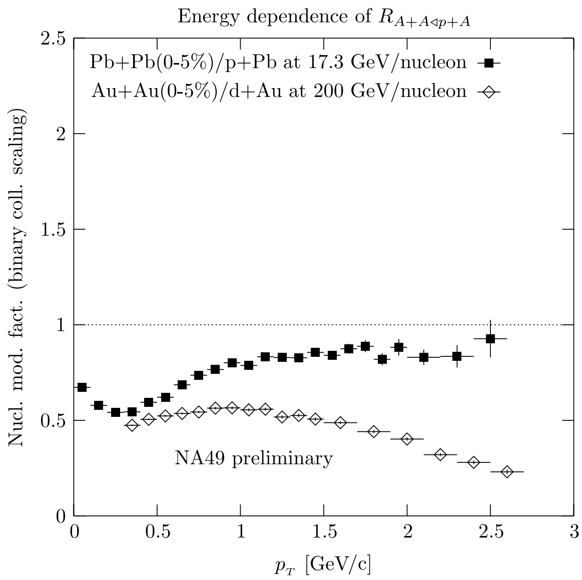

Figure 6. The nuclear modification factor R_{AA} for charged pions at mid-rapidity (-0.3 $< y <$ 0.7) relative to a p+Pb (d+Au) baseline for central Pb+Pb (Au+Au) collisions at $\sqrt{s_{\mathrm{NN}}}$ = 17.3 GeV (200 GeV) as a function of p_{t}.

data as baseline [27, 30] or employ recent p+A data [31, 32] in order to construct a nuclear modification factor:

$$R_{\mathrm{AA}}(p_{\mathrm{t}}) = \frac{\langle N_{\mathrm{coll}}(\mathrm{p+A})\rangle}{\langle N_{\mathrm{coll}}(\mathrm{A+A})\rangle} \frac{\mathrm{d}N_{\mathrm{AA}}/\mathrm{d}p_{\mathrm{t}}}{\mathrm{d}N_{\mathrm{pA}}/\mathrm{d}p_{\mathrm{t}}}. \tag{5}$$

Both approaches provide a larger p_{t} reach than the presently available p+p data at the SPS and have also the benefit of removing to a certain extent the Cronin effect, which is getting stronger towards lower energies and dominates nuclear modifications here [29]. Figure 6 compares R_{AA} from NA49 at the SPS, constructed with p+Pb reference data, to a similar measurement at RHIC, using d+Au as baseline [33]. While the observed R_{AA} values are clearly not as low as at $\sqrt{s_{\mathrm{NN}}}$ = 17.3 GeV than at $\sqrt{s_{\mathrm{NN}}}$ = 200 GeV, there is nevertheless an indication for a small suppression relative to pure binary scaling, in agreement with a recent analysis of π^0 spectra [32]. This might indicate that the mechanisms responsible for the high-p_{t} suppression at RHIC are also already present at SPS.

7. Conclusions

New data on (anti-)proton production at 20A–80A GeV provide insight into the energy dependence of stopping in the region where the onset of deconfinement possibly occurs. No significant energy dependence of $\langle \delta y \rangle / y_{\mathrm{p}}$ is observed. Recent results on the system size dependence of hyperon production allows us to determine the evolution of strangeness enhancement relative to elementary p+p collisions. A first study of global Λ polarization at the SPS is presented. No significant polarization is observed. Results on elliptic flow of strange particles $(\Lambda, \mathrm{K}^0_{\mathrm{S}})$ up to $p_{\mathrm{t}} \approx 2.7$ GeV/c are discussed. Indications for a high-p_{t} suppression are visible at SPS energies in nuclear modification factors using p+Pb data as a baseline.

Acknowledgments

This work was supported by the US Department of Energy Grant DE-FG03-97ER41020/A000, the Bundesministerium fur Bildung und Forschung, Germany, the Virtual Institute VI-146 of Helmholtz Gemeinschaft, Germany, the Polish State Committee for Scientific Research (1 P03B 006 30, 1 P03B 097 29, 1 PO3B 121 29, 1 P03B 127 30), the Hungarian Scientific Research Foundation (T032648, T032293, T043514), the Hungarian National Science Foundation, OTKA, (F034707), the Polish-German Foundation, the Korea Science & Engineering Foundation (R01-2005-000-10334-0) and the Bulgarian National Science Fund (Ph-09/05).

References

[1] Afanasiev S V *et al* (NA49 Collaboration) 1999 *Nucl. Instrum. Meth.* A **430** 210
[2] Alt C *et al* (NA49 Collaboration) 2006 *Phys. Rev.* C **73** 044910
[3] Appelshäuser H *et al* (NA49 Collaboration) 1999 *Phys. Rev. Lett.* **82** 2471
[4] Becattini F *et al* 2006 *Phys. Rev.* C **73** 044905 and private communication
[5] Ahle L *et al* (E802 Collaboration) 1999 *Phys. Rev.* C **60** 064901
[6] Bearden I G *et al* (BRAHMS Collaboration) 2004 *Phys. Rev. Lett.* **93** 102301
[7] Back B B *et al* (E917 Collaboration) 2001 *Phys. Rev. Lett.* **86** 1970
[8] Videbaek F and Hansen O 1995 *Phys. Rev.* C **52** 2684
[9] Petersen H and Bleicher M 2006 *Preprint* nucl-th/0611001 and private communication
[10] Bächler J *et al* (NA35 Collaboration) 1994 *Phys. Rev. Lett.* **72** 1419
[11] Mitrovski M *et al* (for the NA49 Collaboration) 2006 *J. Phys. G: Nucl. Part. Phys.* **32** s43
[12] Alt C *et al* (NA49 Collaboration) 2005 *Phys. Rev. Lett.* **94** 052301
[13] Białas A, Błeszyński M and Czyz W 1976 *Nucl. Phys.* B **111** 461
[14] Antinori F *et al* (NA57 Collaboration) 2006 *J. Phys. G: Nucl. Part. Phys.* **32** 427
[15] Abelev B *et al* (STAR Collaboration) 2007 *Preprint* nucl-ex/0705.3371
[16] Susa T *et al* (for the NA49 Collaboration) 2002 *Nucl. Phys.* A **698** 491
[17] Liang Z and Wang X N 2005 *Phys. Rev. Lett.* **94** 102301
[18] Alt C *et al* (NA49 Collaboration) 2003 *Phys. Rev.* C **68** 034903
[19] Abelev B I (STAR Collaboration) 2007 *Phys. Rev.* C **76** 024915
[20] Stefanek G *et al* (NA49 Collaboration) 2006 *Preprint* nucl-ex/0611003
[21] Huovinen P 2003 *Quark–Gluon Plasma* ed R C Hwa (Singapore: World Scientific) pp 600–33 (*Preprint* nucl-th/0305064) and private communication
[22] Retiere F and Lisa M 2004 *Phys. Rev.* C **70** 044907
[23] Adams J *et al* (STAR Collaboration) 2004 *Phys. Rev. Lett.* **92** 052302
[24] Issah M and Taranenko A 2006 *Preprint* nucl-ex/0604011
[25] Lacey R and Taranenko A 2006 *Preprint* nucl-ex/0610029
[26] Alt C *et al* (NA49 Collaboration) 2006 *Eur. Phys. J.* C **45** 343
[27] Aggarwal M M *et al* (WA98 Collaboration) 2002 *Eur. Phys. J.* C **23** 225
[28] d'Enterria D 2004 *Phys. Lett.* B **596** 32
[29] Blume C 2007 *Nucl. Phys.* A **783** 65c
[30] Laszlo A *et al* (for the NA49 Collaboration) 2006 *Nucl. Phys.* A **774** 473
[31] Laszlo A *et al* (for the NA49 Collaboration) 2007 *Preprint* nucl-ex/0702044
[32] Aggarwal M M *et al* (WA98 Collaboration) 2007 *Preprint* nucl-ex/0708.2630
[33] Adler S S *et al* (PHENIX Collaboration) 2004 *Phys. Rev.* C **69** 034909
Adler S S *et al* (HENIX Collaboration) 2006 *Phys. Rev.* C **74** 024904